Proceedings of the 28th IEEE
EMBS Annual International Conference
New York City, USA, Aug 30-Sept 3, 2006

Impedance Analyzer for *in vivo* Electroporation Studies

Antoni Ivorra and Boris Rubinsky

***Abstract*—Electroporation, the permeabilization of the cell membrane with electrical pulses, is being used for *in vivo* gene therapy, drug therapy and minimally invasive tissue ablation. Applying electrical pulses across cells can have a variety of outcomes; from no effect to reversible electroporation to irreversible electroporation. For reliable *in vivo* use of electroporation it is important to have real time feedback on the outcome of the application of the electrical pulse. Recently, it has been proposed that measuring the electrical properties of electroporated tissues in temporal relation to the applied pulses could provide this feedback. To generate fundamental data on the *in vivo* electrical properties of electroporated tissues we have developed a fast spectroscopic impedance analyzer that measures electrical properties of tissues *in vivo* in conjunction with commercial electroporation pulse generators. Here we describe the apparatus and illustrate its use with an experiment on reversible electroporation in a rat liver.**

I. INTRODUCTION

ELECTROPORATION, or electropermeabilization, is the phenomenon in which cell membrane permeability to ions and macromolecules is increased by exposing the cell to short (microsecond to millisecond) high voltage electric field pulses. While the exact mechanism of permeabilization is not precisely understood experiments show that the application of electrical pulses can have several different effects on the cell membrane, as a function of various pulse parameters; such as amplitude, length, shape, number of repeats and intervals between pulses. As a function of these parameters, the application of the electrical pulse can have no effect, can have a transient permeabilization effect known as reversible electroporation or can cause permanent permeabilization known as irreversible electroporation. Both, reversible and irreversible electroporation have important application in biotechnology and medicine. Reversible electroporation is now commonly used with micro-organisms and cells in culture for transfection and introduction or removal of macromolecules from individual cells. Irreversible electroporation is used for sterilization of liquid media from micro-organisms. During the last decade reversible electroporation has started to be used in living tissues for *in vivo* gene therapy (electrogenetherapy) [1-3] and to enhance the penetration of anti-cancer drugs into undesirable cells (electro-chemotherapy) [4]. Recently, irreversible electroporation has also found a use in tissues as a minimally invasive surgical procedure to ablate undesirable tissue without the use of adjuvant drugs [5, 6].

Successful electroporation, either reversible or irreversible, depends on too many factors to be reliable applied in an open loop procedure, in particular when a yield of close to 100% is desired; such as in the treatment of cancer or when rare cells such as oocytes are treated. It is obvious that for optimal application of electroporation it is desirable to be able to close the open loop with feedback information on the outcome of the applied pulse or pulses.

A possible method for assessing the effects of electroporation is through measurements of the electrical properties of the electroporation affected cells or tissues. A simplistic model of a cell can be used to qualitatively understand the effects of electroporation on the cell electrical properties. In such a model a resistance representing the extra-cellular medium is in parallel with a capacitance accounting for the cell membrane in series with a resistance representing the intra-cellular medium [7]. When electropermeabilization is achieved, then the membrane capacitance is partially shunted by a membrane resistance. Afterwards, resealing of the membrane causes the shunting resistance to increase and the impedance returns to its original values. From these considerations, measuring changes in electrical properties of cells has been proposed for determining the effectiveness of electroporation protocols in individual cells [8, 9] and in cell cultures [10]. Similarly changes in electrical properties were proposed for detecting electroporation in tissues [12], including the creation of images of the electroporated tissue volumes by means of Electrical Impedance Tomography [11, 12].

This study is part of a comprehensive effort to fully characterize the changes in electrical properties of tissue with electroporation. This information should serve as feedback for real time control of the process of electroporation. The first step in the study was to develop an apparatus for multifrequency analysis of the electrical properties of electroporated tissue as a function of time in relation to the electroporation pulses. Here, we will describe the apparatus and illustrate its use with results from a reversible electroporation experiment in the rat liver.

Manuscript received April 3rd, 2006. This work was supported in part by the U.S. National Institutes of Health (NIH) under Grant 5R01RR1459.

Antoni Ivorra is with the University of California at Berkeley, Berkeley, CA 94720, USA (phone: 510-643-1866; (to whom correspondence should be addressed) email: antoni.ivorra@gmail.com).

Boris Rubinsky is with the University of California at Berkeley, Berkeley, CA 94720, USA (phone: 510-643-1866; email: rubinsky@me.berkeley.edu).

II. ELECTRONIC SYSTEM

A. General Architecture

The general architecture of the system is shown in Fig. 1. An electroporation voltage is applied to the sample through a pair of large annular electrodes. The active surfaces of the electrodes are placed in parallel across the tissue sample. The electrical properties of the tissue are measured during and after the application of the electroporation pulse. After the electroporation pulse the impedance of the tissue between the electrodes is measured by using the four-electrode method in which the electroporation electrodes are used as the current injection electrodes and a pair of smaller inner electrodes are used to measure the induced voltage difference across the tissue sample. Recording of current and voltage during the electroporation pulse application is performed with a strategy similar to that described in [10, 13, 14]. Specific to our apparatus is the use of a small sensing resistor (1Ω) for measurements instead of the use of a magnetic based current sensor. We choose to use a resistor rather than magnetic sensors because the sample impedances are expected to be much larger (> 200 Ω) than in the previous studies and the error introduced by restive measurement becomes insignificant when taking into account the typical vertical resolution of oscilloscopes (8 bits).

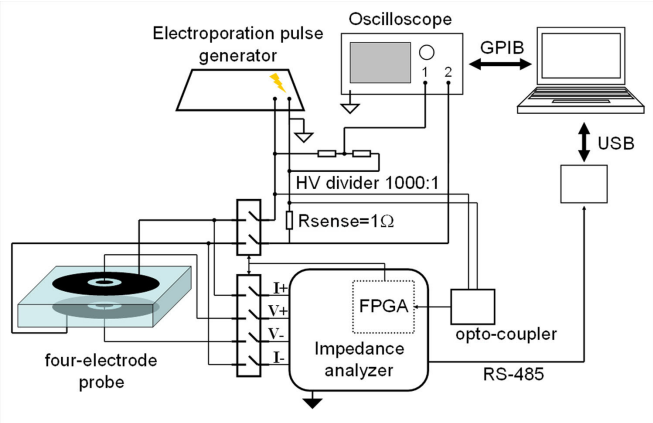

Fig. 1. General architecture of the developed system. The "quasi DC" resistance is recorded by the oscilloscope during the electroporation pulses whereas AC impedance is measured afterwards.

The post pulse impedance measurement is made with a custom developed impedance analyzer that is embedded in a single Printed Circuit Board (PCB) with the rest of components of the system. This subsystem is disconnected from the sample during the pulse application. Otherwise, the electronics would be damaged because of the high voltages applied for electroporation (up to 1500 V). We considered using surge protection mechanisms, as an alternative. However, such protection may have caused distortion of the impedance measurement or the electroporation fields.

Automatic connection and disconnection are performed by means of high-voltage reed relays with switch times below 2ms (MS Series, Meder Electronic AG) that are controlled by the Field Programmable Gate Array (FPGA) that governs the whole system. Initially, the sample is connected to the electroporation pulse generator and disconnected from the AC impedance meter. After a high-voltage (HV) pulse signal is detected and a signal sent to FPGA through an optical-coupler, the system waits for a specified amount of time before connecting the impedance meter.

B. Impedance Analysis module

The impedance analyzer architecture (Fig. 2) is based on previous designs described in [7, 15, 16]. Briefly, an AC signal is generated by using a Direct Digital Synthesizer (DDS) and injected into the sample through a limiting resistor. Then, voltage difference and current signals are collected separately and processed to obtain their real and imaginary parts in relation to a reference signal. Basically, such processing is a digital cross-correlation between the input signals and the reference signal.

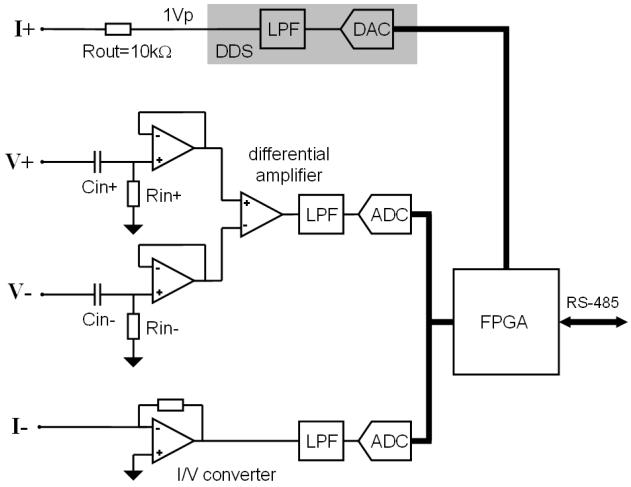

Fig. 2. Schematic representation of the fast impedance analyzer.

The present system includes two novelties. First, as far as the authors know, this is the first impedance analyzer that makes use of a single FPGA (Spartan-3 XC3S200, Xilinx Inc.) to control all the signals and to perform the required digital processing tasks. Typically, two or more fast logic devices are required to manage ADC, DAC and buffer memory signals and a DSP is used to perform processing tasks [17].

The second novelty is that system is able to operate in both, the frequency scan mode and in simultaneous multi-frequency mode. When used in the scan mode, frequencies are sequentially generated and measured. Since five or more cycles are required to reach permanent regime, this mode provides relatively slow rate measurements. For instance, a scan from 1 kHz to 400 kHz with ten frequency points takes approximately 25 ms. When used in the multi-frequency mode, the input signal is an additive combination of multiple sinusoidal signals and the output signals are simultaneously

demodulated for all the generated frequencies. In the multifrequency mode the system is able to measure impedances simultaneously, for instance, at 1 kHz and 15 kHz at a rate of 1000 samples/second.

It is worth to note that the input capacitances (Cin+, Cin- = 1000 nF) at the voltage terminals are not intended for safety reasons but to avoid, or minimize, the saturation of input stages because of DC voltage. In general, any pair of electrodes immersed in an electrolyte will produce some DC voltage in the range of mV. However, in the present case, the application of the electroporation HV pulses, will produce a much larger transient quasi-DC voltage of several tens of mV that will last for some milliseconds.

III. Electrode Setup

Fig. 1 shows the electrode setup in relation to the entire apparatus. It is used for both electroporation and impedance measurement. The electrodes consist of two plates set at a fixed distance in parallel. Figure 3 shows a schematic of the electrodes and their placement. The vertical left line in Fig.3 is the line of symmetry and the figure shows half the plates. Each plate is made of a large external annular electrode for electroporation and current injection (I+, I-) and a smaller circular electrode for voltage detection (V+,V-). Fig 3 also shows a typical electrical field magnitude distribution during the experiment discussed later in this paper. The electrodes were 10 mm in diameter and there was a distance of 5 mm between the electrodes. The voltage that was set across the electroporation electrodes was 225V, which in the experiment were applied in eight 100 μs pulses separated by 100 ms. These pulses were chosen to produce reversible electroporation [5], with values around 450 V/cm. The calculations in the figure show that presence of the inner voltage measurement electrodes distorts the electric field during electroporation when compared to a two disk arrangement. However, as shown in the simulation depicted in Fig. 3, the "shadowed" tissue volume is not significant (<1% of electroporated volume)

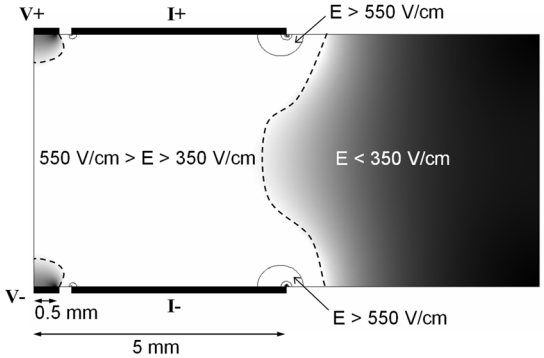

Fig. 3. Finite-element simulation (FEMLAB) of the electric field produced by the probe (axial symmetry). The selected electric field for reversible electroporation is 450 V/cm. (225 V were applied between electrodes I+ and I-). At the electrode edges the field is higher and, presumably, irreversible electroporation or burning will be caused. Under electrodes V+ and V- a shadowed volume appears since current is shunted by these electrodes.

The electroporation plates were produced by using standard Printed Circuit Board technology (Sierra Proto Express Inc., Sunnyvale, CA, USA). FR-4 was selected as the board material and soft bondable gold was selected as finishing for the electrodes.

In order to reduce the electrode-tissue interface impedance, platinum black was deposited with electrochemical deposition on the gold electrodes [18]. Such interface impedance reduction is useful for four-electrode impedance measurements [7]. Here, we have also found that it reduces the magnitude of the electrochemical DC voltage after the application of the HV pulses.

The cell constant, K, defined as the ratio between the resistivity and the measured resistance, will depend on the sample geometry. However, taking into account a range of reasonable expected geometries, finite-element simulations provide a value for $K = 2.76 \pm 0.05$ cm. Experimental measurements with saline solutions give a slightly larger value, K=2.9 cm. The results are evaluated with K=2.8 cm.

IV. Experimental Measurement Methods

Male Sprague-Dawley rats (250-350 g) were obtained from Charles River Labs through the Office of Laboratory Animal Care at the University of California, Berkeley. They received humane care from a properly trained professional in compliance with both the Principals of Laboratory Animal Care and the Guide for the Care and Use of Laboratory Animals, prepared and formulated by the Institute of Laboratory Animal Resources and published by the NIH.

The experiment started with anesthetization of the animal via intraperitoneal injection of Nembutal solution (50 mg/ml sodium pentobarbital, Abbott Labs, North Chicago, IL) for a total of 100 mg sodium pentobarbital per kg of rat. Thirty minutes later, the liver was exposed via midline incision. Then, the electrodes were attached across one lobe of liver and a sequence of square pulses of 225 V and 100 μs at a frequency of 10 Hz was applied with a commercial pulse generator (ECM 830, *Harvard Apparatus*; Holliston, MA) connected to the developed system as shown in Fig.1. The calculated electrical field in the liver is shown in Fig 3.

The system was configured to measure in the multi-frequency mode (1 kHz and 15 kHz) up to 500 ms after the end of last pulse. After this time point, frequency scans (eleven frequencies from 1kHz to 400 kHz) were recorded for 30 minutes.

V. Results and Discussion

Fig. 4 shows typical results obtained with the multifrequency mode after the application of each of the eight 100 μs pulses. The figure shows the impedance measured at 1 kHz and the phase shift measured at 15 kHz. The results are consistent with a decrease of impedance magnitude at low frequencies due to membrane shunting with electroporation. The results also show the membrane

resealing effect of reversible electroporation.

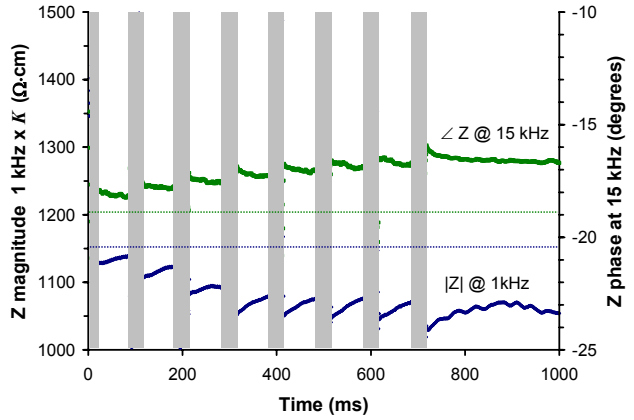

Fig 4. Example of impedance magnitude (|Z|) at 1 kHz and phase angle (∠ Z) at 15 kHz during electroporation burst.

The longer term effects of electroporation are shown in Fig 5. The example depicted in Fig. 5 indicates the presence of a single impedance dispersion manifested over the entire analyzed spectrum (from 1 kHz to 400 kHz) and during all the recorded time. As expected, low-frequency impedance magnitude decreases immediately after the pulses. However, quite surprisingly, it increases afterwards and overcomes the original values before electroporation. Since this fact occurs within the time scale in which reversible blood occlusion is manifested after electroporation [19], it is reasonable to think that both phenomena are linked. A possible explanation could be related to ischemia (blood occlusion) induces cell swelling and, consequent, narrowed extra-cellular paths for low-frequency currents [7]. This type of behavior was found at low frequencies in liver in responses to artificial ischemia (Δ|Z|> 10 % in 1 minute) [20].

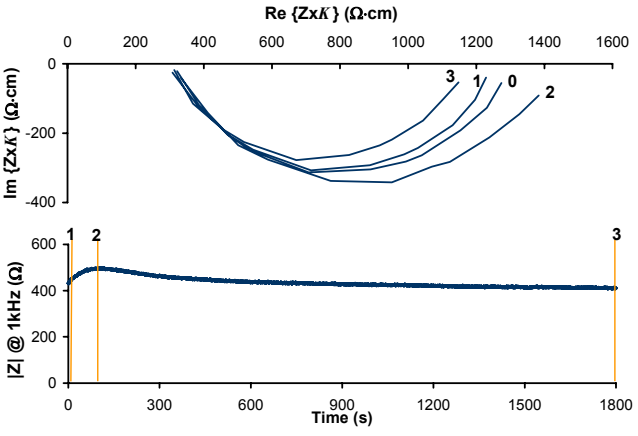

Fig 5. Graph on the top shows impedance locus of impedance at different time points after electroporation that are marked on the bottom graph (0 indicates impedance locus before electroporation).

ACKNOWLEDGMENT

The authors would like to thank Liana Horowitz for her help with animal experimentation.

REFERENCES

[1] M. J. Jaroszeski, R. Heller, and R. Gilbert, *Electrochemotherapy, electrogenetherapy, and transdermal drug delivery: electrically mediated delivery of mollecules to cells*, vol. 37. Totowa, New Jersey: Humana Press, 2000.

[2] D. A. Dean, "Nonviral gene transfer to skeletal, smooth, and cardiac muscle in living animals," *Am J Physiol Cell Physiol*, vol. 289, pp. C233-245, 2005.

[3] L. M. Mir, P. H. Moller, F. Andre, and J. Gehl, "Electric Pulse-Mediated Gene Delivery to Various Animal Tissues," in *Advances in Genetics*, vol. Volume 54: Academic Press, 2005, pp. 83-114.

[4] A. Gothelf, L. M. Mir, and J. Gehl, "Electrochemotherapy: results of cancer treatment using enhanced delivery of bleomycin by electroporation," *Cancer Treatment Reviews*, vol. 29, pp. 371-387, 2003.

[5] R. V. Davalos, L. M. Mir, and B. Rubinsky, "Tissue Ablation with Irreversible Electroporation," *Annals of Biomedical Engineering*, vol. 33, pp. 223, 2005.

[6] L. Miller, J. Leor, and B. Rubinsky, "Cancer cells ablation with irreversible electroporation," *Technology in Cancer Research and Treatment*, vol. 4, pp. 699-706, 2005.

[7] A. Ivorra, "Contributions to the measurement of electrical inpedance for living tissue ischemia injury monitoring," in *Electronic Eng. Dept.*, vol. PhD. Barcelona: Universitat Politècnica de Catalunya, 2004.

[8] Y. Huang and B. Rubinsky, "Micro-electroporation: improving the efficiency and understanding of electrical permeabilization of cells," *Biomedical Microdevices*, vol. 3, pp. 145-150, 1999.

[9] B. Rubinsky and Y. Huang, "Controlled electroporation and mass transfer across cell membranes, US patent 6300108," 2001.

[10] M. Pavlin, M. Kanduser, M. Rebersek, G. Pucihar, F. X. Hart, R. Magjarevic, and D. Miklavcic, "Effect of Cell Electroporation on the Conductivity of a Cell Suspension," *Biophysical Jounal*, vol. 88, pp. 4378-4390, 2005.

[11] B. Rubinsky and Y. HUang, "Electrical Impedance Tomography to control electroporation, US patent 6,387,671," 2002.

[12] R. V. Davalos, B. Rubinsky, and D. M. Otten, "A Feasibility Study for Electrical Impedance Tomography as a Means to Monitor Tissue Electroporation for Molecular Medicine," *Biomedical Engineering, IEEE Transactions on*, vol. 49, pp. 400-403, 2002.

[13] L. F. Cima and L. M. Mir, "Macroscopic characterization of cell electroporation in biological tissue based on electrical measurements," *Applied Physics Letters*, vol. 85, pp. 4520-4522, 2004.

[14] U. Pliquett, R. Elez, A. Piiper, and E. Neumann, "Electroporation of subcutaneous mouse tumors by trapezium high voltage pulses," *Bioelectrochemistry*, vol. 62, pp. 83-93, 2004.

[15] T. Dudykevych, E. Gersing, F. Thiel, and G. Hellige, "Impedance analyser module for EIT and spectroscopy using undersampling," *Physiological Measurement*, vol. 22, pp. 19-24, 2001.

[16] B. Rigaud, J. P. Morucci, and N. Chauveau, "Bioelectrical impedance techniques in medicine. Part I: Bioimpedance measurement. Second section: impedance spectrometry," *Critical Reviews in Biomedical Engineering*, vol. 24, pp. 257-351, 1996.

[17] R. Halter, A. Hartov, and K. D. Paulsen, "Design and implementation of a high frequency electrical impedance tomography system," *Physiological Measurement*, vol. 25, pp. 379-390, 2004.

[18] L. A. Geddes, *Electrodes and the measurement of bioelectric events*. New York: Wiley-Interscience, 1972.

[19] J. Gehl, T. Skovsgaard, and L. M. Mir, "Vascular reactions to in vivo electroporation: characterization and consequences for drug and gene delivery.," *Biochimica et Biophysica Acta*, vol. 1569, pp. 51-58, 2002.

[20] D. Haemmerich, O. R. Ozkan, J. Z. Tsai, S. T. Staelin, S. Tungjitkusolmun, D. M. Mahvi, and J. G. Webster, "Changes in electricel resistivity of swine liver after occlusion and postmortem," *Medical & Biological Engineering & Computing*, vol. 40, pp. 29-33, 2002.